Analysis of waveguide-splitter-junction in high-index Silicon-On-Insulator waveguides

Damian Goldring[*], Evgeny Alperovich[*], Uriel Levy[**] and David Mendlovic[*]

[*] *Faculty of Engineering, Tel Aviv University, 69978 Tel Aviv, Israel*
[**] *Dep. Of Electrical & Computer Engineering, University of California, San Diego, 9500 Gilman Drive, La Jolla, CA 92093-0407*

goldrin@post.tau.ac.il

Abstract: We propose and analyze a new type of four ports structure for ultra-compact waveguide splitting. This structure differs from most existing ultra-compact waveguide splitters by introducing complete symmetry between the input and output ports. Maximum overall throughput predicted is ~81% where reflection and crosstalk are <1%. A 2D photonic-crystal implementation concept. Is presented as well. Concept of operation and simulation results are provided. The trade-off between performances and functionality is discussed.

OCIS codes: (130.3120) Integrated optics devices; (230.1360) Beam splitters

References and Links

1. See http://jdj.mit.edu/, http://nanophotonics.ece.cornell.edu/research.html, http://www.its.caltech.edu/%7Eaphyariv/base.html
2. S. McNab, N. Moll, Y. Vlasov, "Ultra-low loss photonic integrated circuit with membrane-type photonic crystal waveguides," Opt. Express **11**, 2928-2939 (2003)
3. J. S. Forsei, P. R. Villeneuve, J. Ferrara, E. R. Thoen, G. Steinmeyer, S. Fan, J. D. Joannopoulos, L.C kimerling, H. I. Smith, E. P. Ippen, "Photonic-bandgap microcavities in optical waveguides," Nature **390**, 143-145 (1997)
4. V. Almeida, R. Panepucci, M. Lipson, "Nanotaper for compact mode conversion," Opt. Lett. **28,** 1302-1304 (2003)
5. Y. Vlasov, S. McNab, "Losses in single-mode silicon-on-insulator strip waveguides and bends," Opt. Express **12**, 1622-1631 (2004)
6. A. Sakai, G. Hara, T. Baba, "Propagation characteristics of ultrahigh-Δ on silicon-on-insulator substrate," Jap. J. App. Phy. **40**, L383-385 (2001)
7. C. Manolatou, S. G. Johnson, S. Fan, P. R. Villeneuve, H. A. Haus and J. D. Joannopoulos, "High density integrated optics," J. Lightwave Technol. **17**, 1682-1692 (1999)
8. R. L. Espinola, R. U. Ahmad, F. Pizzuto, M. J. Steel, R. M. Osgood, "A study of high-index contrast 90^0 waveguide bend structures," Opt. Express **8**, 517-528 (2001)
9. R. U. Ahmad, F. Pizzuto, G. S. Camarada, R. L. Espinola, H. Rao, R. M. Osgood, "Ultra-compact corner mirrors and T-branches in silicon-on-insulator," IEEE Photon. Technol. Lett. **14**, 65-67 (2002)
10. T. Fukazawa, T. Hirano, F. Ohno, T. Baba, "Low loss intersection of Si photonic wire waveguides," Jap. J. App. Phy. **43**, 646-647 (2004)
11. C. Chen, H. Chien, P.G. Luan, "Photonic crystals beam splitters," App. Opt. **43**, 6187-6190 (2004)
12. L.H. Frandsen, W. Bogarets, V. Wiaux, "Ultralow-loss 3dB photonic crystal waveguide splitter," Opt. Lett. **29**, 1623-1625 (2004)
13. X. Yu, S. Fan, "Bends and splitters for self-collimated beams in photonic-crystals," App. Phy. Lett. **83**, 3251-3253 (2003)
14. D. Pustai, S. Shi, C. Chen, A. Sharkawy, D. Prather, "Analysis of splitters for self-collimated beams in planar photonic crystals," Opt. Express **12**, 1823-1831 (2004)
15. S. G. Johnson, C. Manolatou, S. Fan, P. R. Villeneuve, H. A. Haus and J. D. Joannopoulos, "Elimination of cross talk in waveuide intersections," Opt. Lett. **23**, 1855-1857 (1998)
16. M. Tinkham, *Group theory and quantum mechanics*, (McGraw-Hill, New York, 1964).
17. See www.rsoftdesign.com

1. Introduction

High-index based integrated optical devices are attracting growing attention mainly due to their high field localization capabilities offering the advantage of dense on-chip integration[1]. During the past decade, high index based waveguides[2], resonators[3], couplers and various other devices[4] have been suggested and demonstrated. One of the most common material systems used for high-index integrated optics is the Silicon-On-Insulator (SOI)[5,6]. The combination of useful electronic properties, established fabrication processes and strong light confinement makes it a very promising candidate for the next generation photonic chips.

One of the challenges in high-index integrated photonics is the construction of efficient ultra-compact bends and light splitting junctions. This task has been confronted by several researchers in the past years. Manolatou[7] *et al.* suggested resonant structures for 90^0 bending and splitting of light as well as low crosstalk waveguides intersections. The simulation results predicted ultra-low losses over wide frequency range. Espinola[8] *et al.* suggested a slightly different configuration for 90^0 bends obtaining similar performances. This configuration was also demonstrated experimentally[9]. Another interesting configuration for low crosstalk intersection was presented by Fukazawa[10] *et al.*, where an elliptical resonator that was formed at the junction region almost cancelled the crosstalk. Splitters and curves were also demonstrated in photonic-crystals based structures[11] that produce ultra-high confinement of the light. An optimized photonic-crystal splitter was recently demonstrated by Frandsen[12] *et al.* where the radii of the holes were modified in the vicinity of the junction.

A common property of all the splitting structures mentioned above is the non-symmetric relation between the input and output ports, i.e., the input and the output ports are well-defined and cannot be exchanged. As a counter example, a device with symmetric input-output relation is the well known cubic beam splitter. The question is whether a similar device can be implemented with high-index, ultra-compact optical structures. Yu[13] *et al.* and Pustai[14] *et al.* have proposed and demonstrated such devices by using self-collimated beams in photonic crystals. In this paper we propose a new configuration for an integrated optics beam splitter having input-output symmetry relation. The device consists of four ports, each capable of being utilized as an input or output port. Unlike the devices presented in Ref. 13,14 our device utilizes waveguides rather than self-collimated beams. Thus, the issue of coupling between the junction and its input-output waveguides is eliminated. Moreover, much smaller junction area is obtained with our device.. Some insight about the concept of operation is presented in the next section. In section 3 a constant wave (CW) analysis and spectral analysis are presented. Discussion is given in section 4, and section 5 concludes the paper.

2. Concept of operation

The Waveguide-Splitter-Junction (WSJ) is the integrated optics analog of the very well known, free space Beam Splitter (BS). The functionality of the WSJ is essentially identical to that of the BS, however, the electro-magnetic analysis is substantially different.

Figure 1 shows a schematic description of the WSJ. An input beam propagating through port #1 will split equally between ports #2 and #3. The WSJ has complete symmetry along the axis defined by the air slit located in the center of the waveguides intersection and along its perpendicular axis. Therefore, each port can be used as the input port splitting the input beam into the appropriate two other ports. The orientation of the air slit determines which of the two perpendicular ports will be the second output port along with the forward directing port. Some insight about the coupling behavior may be derived from the modes analysis presented by Johnson[15] *et al.* for a regular waveguides crossing. The regular waveguide crossing structure has a C_{4v} symmetry[16], and therefore only one possible two-dimensional irreducible representation exists for the optical modes in the junction. Thus, for a particular optical wavelength the crossing will support two degenerate modes that by interfering enable ultra low crosstalk.
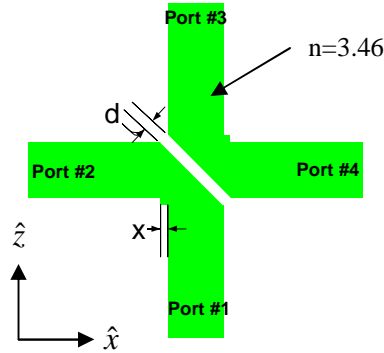
Fig. 1. (a) WSJ structure scheme. Filled area (Green) indicates that the refractive index is n=3.46 while the background index is taken as n=1.

In order to convert the functionality of the simple waveguides crossing into the desired functionality of the WSJ, we have broken the C_{4v} symmetry by creating the diagonal air slit. As a result, a C_{2v} symmetry which has only one-dimensional irreducible representations is now created[16]. By examining this symmetry (see Fig. 2) one can see that it will be impossible to implement the WSJ functionality using only a single C_{2v} resonant mode. However, since the resonant modes have sufficiently low-Q due to the low silicon-to-air reflection coefficient, one can obtain the desired functionality by interfering two of the modes at an off-resonance frequency. The low-Q function maintains the radiation losses at the interfering point sufficiently low in spite the fact that it is an off-resonance frequency. For example, combining the A2 symmetry mode (see Fig. 2) with either one of the B modes (1,2) may provide the desired result. Controlling the junction's parameters and consequently its resonant behavior will enable tuning its spectral response and eventually producing the 3dB power splitting. Note that small rectangular resonators were added in two corners of the junction for that purpose. By controlling the resonators dimensions one can shift the resonant frequency of the modes, thus enabling optimization of the structure (see next section).
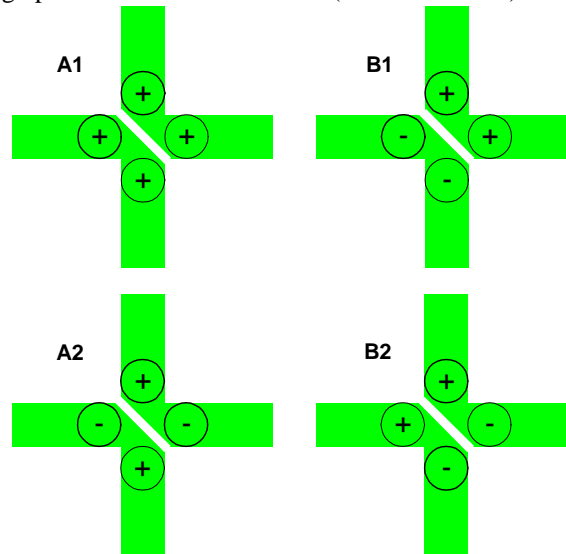

Fig. 2. Schematic description of the symmetry of the possible resonant modes in the WSJ.

In addition to the waveguide-based device we also suggest a Photonic Crystal WSJ (PC-WSJ) configuration which obtains reduced lateral radiation losses[†]. The principle of operation of the two devices is quite similar. In order to build a 90^0 cross junction we had to use a square-lattice photonic crystal. Square lattices are more likely to be used with the rods configuration, i.e., an array of silicon rods, since it enables the formation of single-mode waveguides for a large frequency range. However, the rods configuration generates an air guided mode that is practically impossible to confine in the third (vertical) dimension. Thus, we have chosen to use a holes square lattice for the PC-WSJ. The lattice period was tuned to produce single mode guidance of the waveguides around 1.55μm wavelength and the wavelength range is about 0.09μm. The index contour map of the PC-WSJ is presented in Fig. 3. The array's period is 0.775μm and the holes diameter is 0.68μm. Note that the air slit is now positioned between the two appropriate junction corner holes and that the other two junction corner holes were removed. The removed holes are equivalent to the small resonators added to the WSJ. The symmetry that exists in the WSJ is preserved. It should be mentioned that Chen[11] *et al*. have suggested a similar device concept based on a circular defect instead of an air slit. Unfortunately, in order to get optimized results they had to give up the complete symmetry property. Moreover, the design is based on rods structure rather than holes which has the vertical confinement problem as mentioned above.
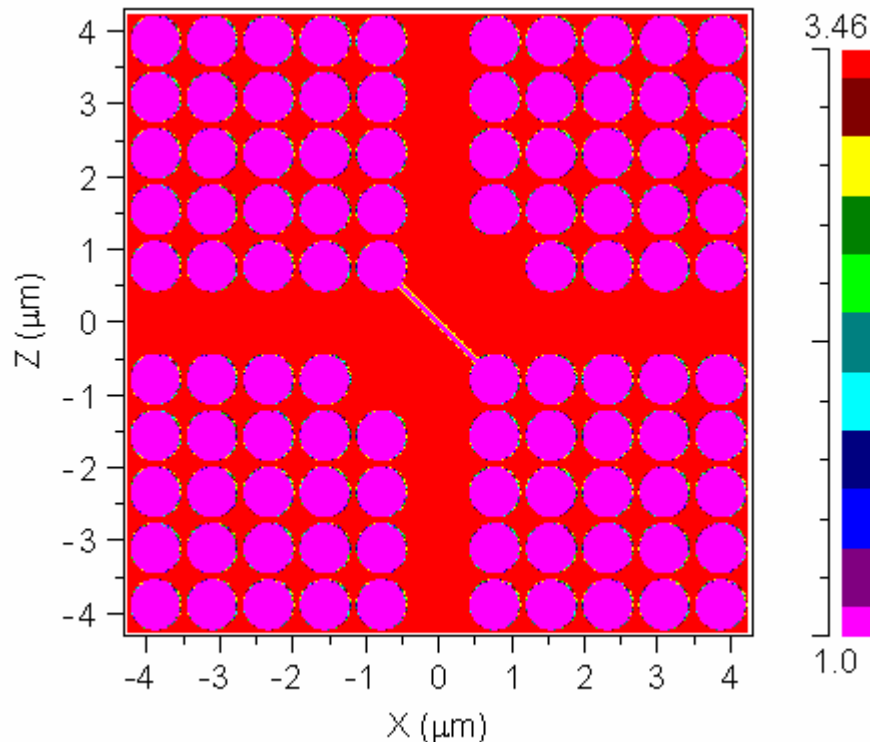

Fig. 3. Refractive index contour map of the PC-WSJ.

[†] Note that radiation losses in the vertical direction of a true 3D structure are not taken into account. These losses will definitely have an effect on the structure's throughput. The calculation of these losses and performing structure optimization for reducing them are beyond the scope of this work.

3. Computer simulations

We used a Finite-Differences-Time-Domain (FDTD) based commercial tool[17] for the evaluation of the electro-magnetic fields. Both CW and pulse analysis were performed for structure optimization and for frequency response calculations. For effective index calculations we used the Beam Propagation Method (BPM). Since the smallest feature size was on the order of 100nm, a 10nm scale was used for the spatial grid. The grid size imposed a maximal time step of $2.33 \cdot 10^{-2}$ fs. For the frequency analysis one wavelength long pulses were used. The waveguides used for the simulations were 450nm wide and their effective refractive index was set to 2.881. This effective index is obtained for a 240nm SOI slab where the SiO_2 refractive index is taken as 1.46 and the Si index as 3.46. Such waveguides support single in-plane polarized (TE) mode in our spectrum of interest (1450nm-1650nm). The former effective index was used also for the 2D simulation of the PC-WSJ indicating that the same SOI slab was used for the PC-WSJ.

Several simulations of the WSJ and PC-WSJ were performed to explore the performance of the devices. The WSJ structure that was used for the simulations is presented in Fig. 1. Figure 4 describes the basic operation of the device (*x=50*nm and *d=56*nm) by showing the distribution of the $\hat{y}$ polarization component of the magnetic field generated by a TE (in-plane) polarized 1.55μm CW source at port #1. One can see that most of the optical field is split between ports #2 and #3. Some of the optical field is radiated outside of the structure and only a small fraction is coupled to ports #4 and #1. We denote the optical power coupled into ports #2 and #3 as *left turn* and *forward throughput*, respectively and the power coupled into ports #4 and #1 as *crosstalk* and *reflection*, respectively.
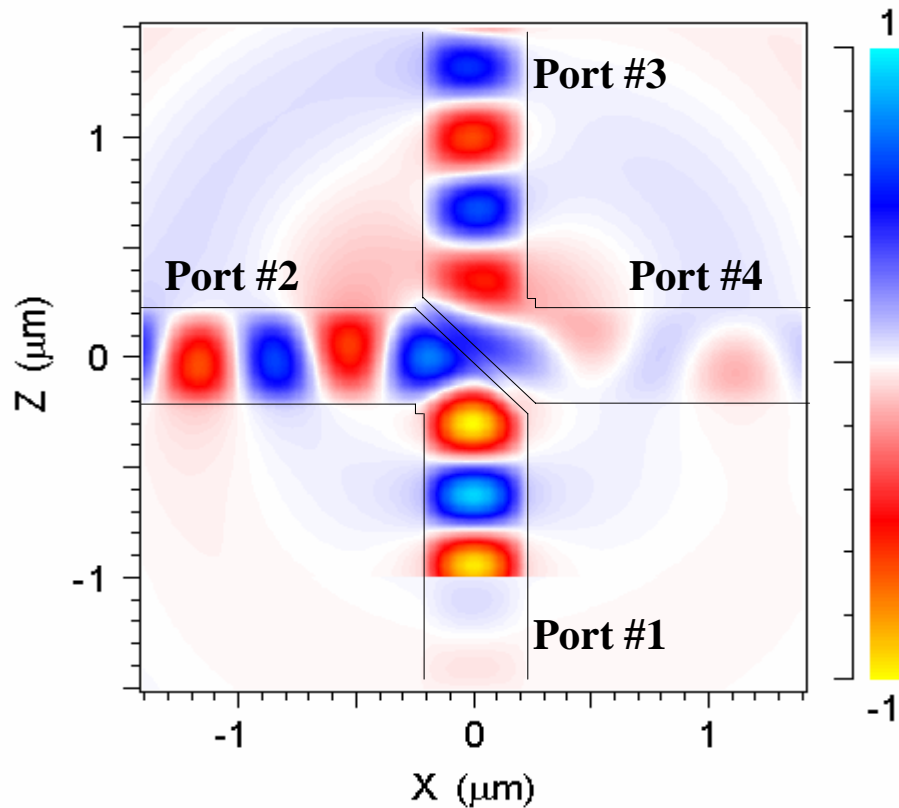

Fig. 4. $\hat{y}$ polarized magnetic field distribution in the WSJ for 1.55 microns CW source. The color-map indicates the field's normalized amplitude.

Figure 5(a-c) presents the spectral characteristics of the WSJ for different resonators dimensions – *x* (see Fig. 1). Although the left turn throughput and the forward throughput, peak at different frequencies, they intersect at a specific frequency in which the throughput is equal at both output ports. We refer to that intersection point as the *equal throughput point*. It is clear that increasing the resonator size increases the overall throughput of the left turn waveguide, thus changing the wavelength and throughput at the equal throughput point.

Figure 5(d) shows the reflection and crosstalk spectral analysis for *x*=50nm. Both signals are on the order of 1%. The results remain similar for variation of *x*. Since in practice the device is a three dimensional structure, a 3D simulation was performed for the optimal configuration of the WSJ, i.e., *x=50*nm and *d=56*nm. The results are presented in Fig. 6. One can see that the equal throughput point wavelength and throughput match the results obtained in the 2D simulations. The whole 3D frequency response is not identical to the 2D one; however, the deviations are small and occur away from the equal throughput point frequency.
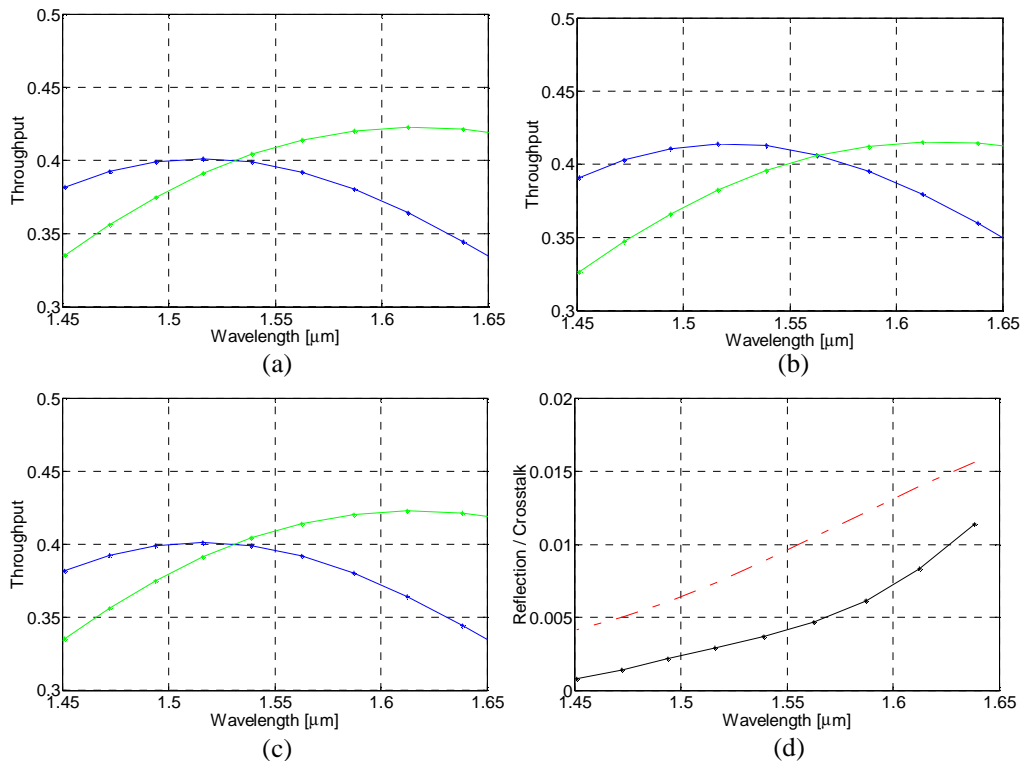

Fig. 5. (a-c) present throughput spectral analysis of the WSJ. (a) *x*=40nm (b) *x*=50nm (c) *x*=60nm and *d*=56nm in all insets. Blue dashed-dotted line is the left turn throughput (port #2) and the green solid-asterick line is the forward throughput (port #3). (d) presents the reflection and crosstalk spectral analysis for *x*=50nm. Red dashed-dotted line is the right turn throughput, i.e., crosstalk (port #4) and the green solid-asterick line

Figure 7 presents the throughput and wavelength at the equal throughput point for different resonator sizes. The equal throughput point wavelength can be shifted within a wide range without a substantial change in throughput by altering the resonators width. Shifting of the equal throughput point wavelength can be achieved also by changing the air slit width. The overall effect of the slit width variation is similar to the effect of resonator dimension variation; however, the sensitivity is different. This can be seen in Fig. 8 showing the throughput (a) and the wavelength (b) at the equal throughput point for different slit widths.
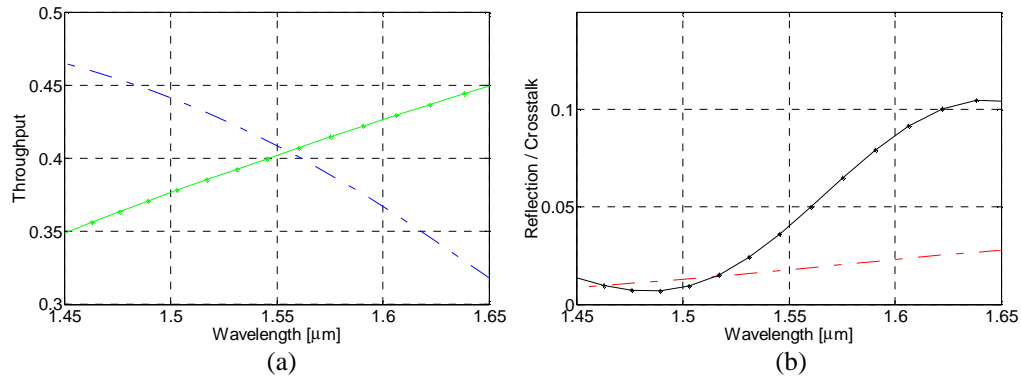
Fig. 6. 3D Spectral analysis of the WSJ. (a) Left turn (blue dashed-line) and forward (green line-asterick) throughput (b) Crosstalk (red dashed-line) and reflection (black line-asterick).
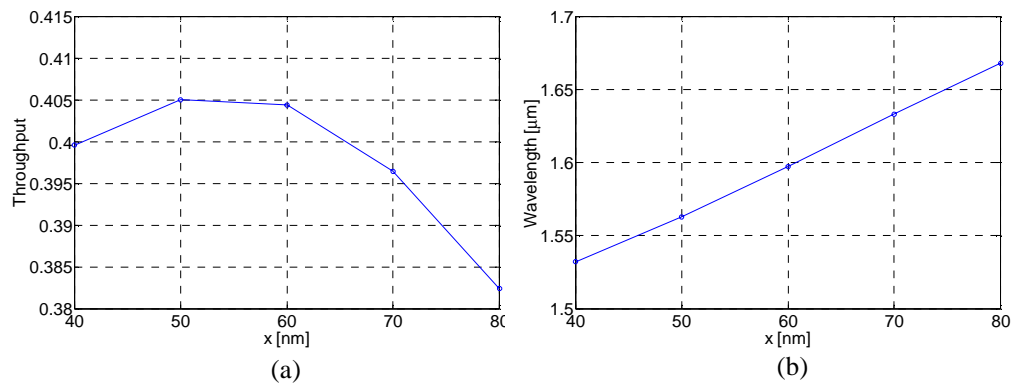

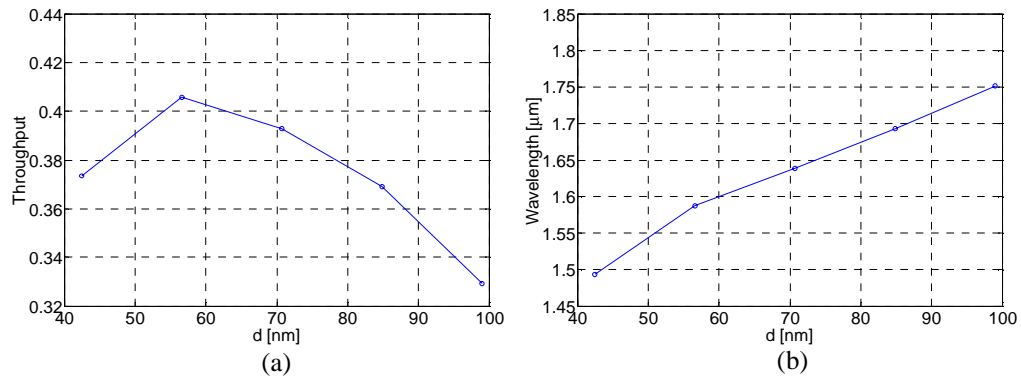Fig. 7. Single port throughput at equal throughput point and Wavelength of equal throughput point Vs. resonator size - *x* .

Fig. 8. Single port throughput at equal throughput point and Wavelength of equal throughput point Vs. slit size - *d* .

The overall throughput of the proposed device is slightly higher than 80%, meaning that ~1 dB losses are unavoidable. To reduce the loss of the proposed device we next present a photonic-crystal based implementation of the WSJ. The highly reflective nature of the photonic-crystal enables the reduction of the radiation loss and increases the overall throughput. Notice that this is true disregarding the vertical radiation losses that occur in the

true 3D structure (see footnote in section 2). The refractive index contour of the PC-WSJ (see Fig. 3) consists of a photonic crystal holes substrate with two intersecting waveguides that were introduced by removing the corresponding lines of holes. In addition there are two missing holes in the junction that are equivalent to the small resonators of the regular WSJ.
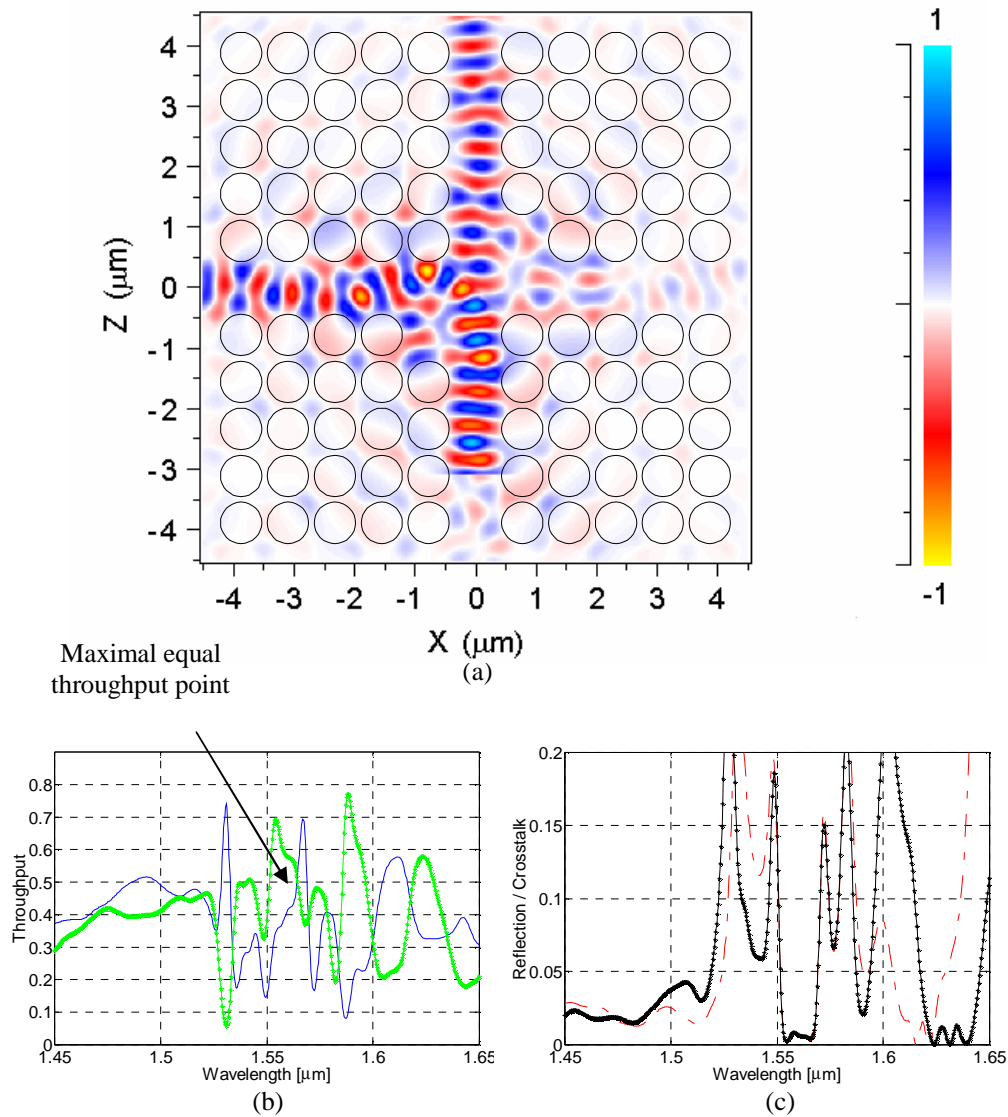

Fig. 9. (a) $\hat{y}$ polarization magnetic field in the PC-WSJ structure for 1.56µm CW source. The color-map indicate the field's normalized amplitude. (b) Left turn (blue solid line) and forward (green line-asterick) throughput spectrum. (c) Crosstalk (red dashed - dotted) and reflection (black line-asterick) spectrum. Air slit thickness is 60nm.

Figure 9(a) depicts the basic operation of the device by showing the $\hat{y}$ polarized magnetic field distribution generated by an in-plane polarized (TE) 1.56µm CW source at port #1. Fig. 9 (b,c) show the spectral characteristics of the PC-WSJ with a 60nm thick air slit. The maximal equal throughput point is shown by the arrow. The inaccuracy of the simulation results due to reflection from boundaries can be up to 5% (varies with wavelength). While the effect of the simulation inaccuracy is negligible for the interesting regions of the crosstalk / reflection

results it is notable for the forward and left turn throughput. The spectral behavior of the PC-WSJ is substantially different from the regular WSJ due to the resonant nature of the photonic crystal. One can see that the 3dB split at the equal throughput point rapidly changes as we move away from the point's wavelength. The reflection and crosstalk are also highly sensitive and are kept low only for a wavelength range of about 20nm.

4. Discussion

In the previous section we have presented several simulation results showing the expected performances of the proposed WSJ devices. Both the WSJ and the PC-WSJ are completely symmetric, i.e., a waveguide mode propagating into the junction from any of its four ports will split into two equal modes at the appropriate ports. We now discuss the results and their implications.

For the WSJ with optimal values of x=50nm and d=56nm (Fig. 5) the reflected energy and the energy coupled to the crosstalk channel are kept below 0.5% and 1% of the incident energy respectively and the overall loss is 0.92dB. While the loss is high compared with other suggested splitters[7,8], it is still within the limits of reason for several applications in which the symmetry property is essential. The results of the 3D simulation show very good agreement with the 2D simulation results. This implies that the radiation loss is mainly in the in-plane direction and the light remains vertically highly confined within the structure.

The results show that the WSJ is wavelength sensitive leading to different throughput in each of the output channels as well as decrease in the overall throughput as the equal throughput point wavelength shifts. Figure 10 emphasizes the last observation by plotting the overall throughput and output channels power ratio versus the optical wavelength for the optimal configuration mentioned above. Evidently, the WSJ cannot be used in applications that require constant throughput over a wide wavelength range; however, the overall throughput across most of the C- band (1530-1565 nm) is kept above 80%, making the device suitable of optical communication applications.
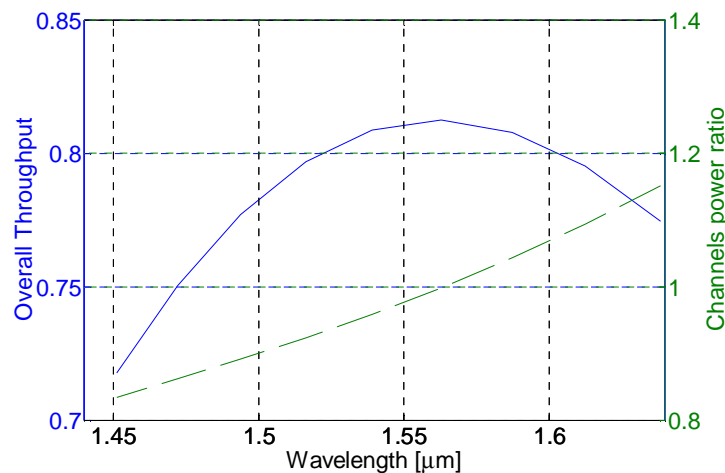

Fig. 10 - Overall throughput of both output ports of the WSJ (Blue line – left axis) and their power ratio (green dashed line – right axis) Vs. wavelength. The resonator size, x=50nm and the slit width, d=56nm.

Since it is most likely that the WSJ will be used to split the energy equally it is of high interest to be able to tune the *equal throughput point* to the desired wavelength of operation. Figure 7 and Figure 8 present the relevant information needed to adjust the *equal throughput point* along the wavelength axis. We see that both x and d can be tuned to yield the desired frequency. We note that for a wavelength range of about 0.2µm the overall throughput decrease can reach as high as 0.65dB (1.57dB in total). In order to slightly overcome this issue one can optimize the sizes of x and d simultaneously to achieve better results.

Potential applications for the WSJ can vary from light energy splitting for telecommunication or computing to building ultra-compact Mach-Zehnder interferometers for nano-scale materials experiments and bio-sensors. Obviously, the relatively high loss and the strong wavelength dependence limit its usefulness for telecommunications systems. The problem might be partially overcome for specific applications by using the PC-WSJ. The photonic-crystal configuration might yield lower loss. The results in Fig. 9 predict <0.23dB losses which are about a quarter of the losses in the regular WSJ. The reflection and crosstalk predicted are <0.01%. However, these calculations neglect the vertical losses and also wavelength sensitivity is now larger due to the high-Q resonators. An optimization of the structure for obtaining low vertical radiation losses is still required.

Fabrication of the WSJ and PC-WSJ is within the current machinery limits. While most of the features dimensions are well above the current fabrication limitations (for example, 450nm waveguides or the holes array photonic crystal), the air slit and the small resonators are of the order of 50nm – 100nm and are of a greater challenge for realization.

5. Conclusions

This paper presented two new types of structures for ultra-compact optical waveguides splitting with symmetry between its input and output ports using high-index semiconductor. One structure (WSJ) is implemented by standard ridge waveguides, while the other (PC-WSJ) is based on photonic crystal implementation. The suggested WSJ functionality is similar to the cubic beam splitter commonly used in free space optics. We analyzed the performances of the proposed devices using finite difference time domain computer simulations. The proposed WSJ devices can be used in large variety of applications, ranging from optical communication to sensing and detection. .

Acknowledgments